Published in final edited form as:

Arterioscler Thromb Vasc Biol. 2020 October ; 40(10): 2425–2439. doi:10.1161/ATVBAHA.120.315003.

Loss of Down syndrome critical region-1 mediated hypercholesterolemia accelerates corneal opacity via pathological neo-vessel formation

Masashi Muramatsu[1,*], **Suguru Nakagawa**[2,4,*], **Tsuyoshi Osawa**[3,*], **Tetsuya Toyono**[4], **Akiyoshi Uemura**[5], **Hiroyasu Kidoya**[6], **Nobuyuki Takakura**[6], **Tomohiko Usui**[4], **Sandra Ryeom**[7], **Takashi Minami**[1]

[1]Div. Molecular and Vascular Biology, IRDA, Kumamoto University, 860-0811 Japan

[2]Div. Genome science, RCAST, the University of Tokyo, 153-8904 Japan

[3]Integrative Nutriomics, RCAST, the University of Tokyo, 153-8904 Japan

[4]Dept. Ophthalmology, Graduate School of Medicine, the University of Tokyo, 113-0033 Japan

[5]Dept. Retinal Vascular Biology, Nagoya City University Graduate School of Medical Sciences, 467-8601 Japan

[6]Dept. Signal transduction, RIMD, Osaka University, 565-0871 Japan

[7]Dept. Cancer Biology, University of Pennsylvania, 19104, USA

Abstract

Objective-—The calcineurin-nuclear factor for activated T cells (NFAT)-Down syndrome candidate region (DSCR)-1 pathway plays a crucial role as the downstream effector of VEGF-mediated tumor angiogenesis in endothelial cells. A role for DSCR-1 in different organ microenvironment such as the cornea and its role in ocular diseases is not well understood. Corneal changes can be indicators of various disease states and are easily detected through ocular examinations.

Approach and Results-—The presentation of a corneal arcus or a corneal opacity due to lipid deposition in the cornea often indicates hyperlipidemia and in most cases, hypercholesterolemia. Although the loss of Apolipoprotein (Apo) E has been well characterized and is known to lead to elevated serum cholesterol levels, there are few corneal changes observed in *ApoE*$^{-/-}$ mice. In this study, we show that the combined loss of ApoE and DSCR-1 leads to a dramatic increase in serum cholesterol levels and severe corneal opacity with complete penetrance. The cornea is normally maintained in an avascular state; however, loss of *Dscr-1* is sufficient to induce hyper-inflammatory and -oxidative condition, increased corneal neovascularization, and lymphangiogenesis. Furthermore, immunohistological analysis and genome-wide screening

Address all correspondence to: Takashi Minami, Ph.D., Div. Molecular and Vascular Biology, IRDA Kumamoto University, 860-0811 Phone: +81-96-373-6500 Fax: +81-96-373-6503 t-minami@kumamoto-u.ac.jp.

*contributed equally

Disclosures

None

revealed that loss of *Dscr-1* in mice triggers increased immune cell infiltration and upregulation of stromal derived factor (SDF)-1 and its receptor, CXCR4, potentiating this signaling axis in the cornea, thereby contributing to pathological corneal angiogenesis and opacity.

Conclusions-—This study is the first demonstration of the critical role for the endogenous inhibitor of calcineurin, DSCR-1 and pathological corneal angiogenesis in hypercholesterolemia induced corneal opacity.

Graphical Abstract

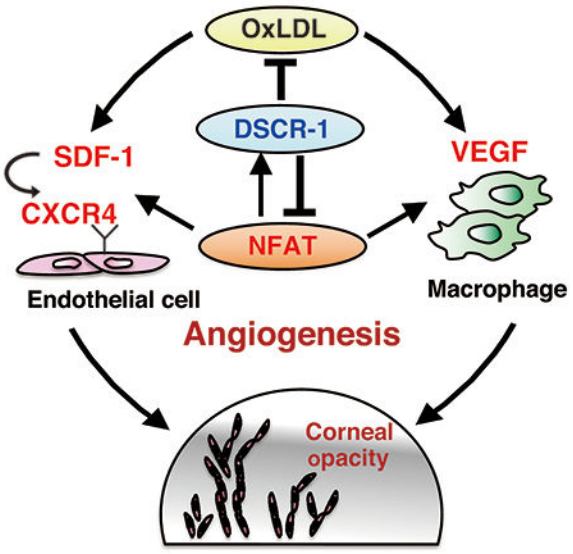

Keywords

Angiogenesis; DSCR-1; corneal opacity; SDF-1; oxLDL; CXCR4; Angiogenesis; Vascular Biology

Introduction

The endothelium is a highly malleable cell layer that constantly senses and responds to changes in the extracellular microenvironment. Most extracellular mediators controlled the epigenetic states, resulting the genes activation or silencing in endothelial cells, which in turn leads to various phenotypic changes, such as cell migration, cell proliferation, angiogenesis, coagulation, and inflammation. Tight control of these processes is essential for maintaining homeostasis. Endothelial cell activation, if excessive, over-sustained, or spatially and temporally misplaced, can lead to vasculopathic conditions, such as pathological angiogenesis, clot formation, and atherosclerosis [1–3]. Thus, understanding the molecular mechanisms and signaling pathways underlying vascular diseases can lead to the identification of new therapeutic targets.

The VEGF-NFAT signaling pathway is a key regulatory pathway involved in inflammation and pathological angiogenesis of the endothelium and is highly associated with pathogenesis during sepsis mortality, tumor growth, and tumor metastasis [4–6]. In addition to VEGF and

the VEGF receptor system, several G-protein coupled receptors also activate endothelial cells by dynamically sensing attractive/repulsive chemokines, such as SDF-1 (also known as CXCL12) and thrombin. The receptors CXCR4/7 and Protease activated receptor1/2 are expressed in endothelial cells during vascular formation, as well as during pathological angiogenesis or the inflammatory process, which in turn affects the vascular motility, integrity, and permeability [7–9].

The Down syndrome candidate region (DSCR)-1 (also known as RCAN1, MCIP-1, calcipressin-1, or Adapt78) is a NFAT-induced feedback modulator of the calcineurin-NFAT pathway. DSCR-1 plays a crucial role in regulating endothelial cell activation and maintaining vascular homeostasis [7, 10]. Improper regulation of the NFAT-DSCR-1 feedback pathway through loss or overexpression of DSCR-1 inhibits endothelial cell activation and ultimately leads to tumor angiogenesis during primary tumor growth, pre-metastatic niche formation, and subsequent tumor metastasis to the lungs, which is mediated by two different mechanisms [11–14]. Besides tumor growth and metastasis, the organ microenvironment also influences vascular bed-specific endothelial cell activation. Under normal conditions, the cornea maintains avascular microenvironment to preserve transparency [15, 16]. However, the primary role of DSCR-1 in corneal angiogenesis is not fully understood. Moreover, to our knowledge, mechanistic basis of how inflammation and hypercholesterolemia lead to corneal opacity are not well studied to date.

Corneal opacity is one of the main causes of blindness, and millions of patients worldwide suffer from this condition. Corneal opacity can be triggered by various stressors that cause inflammation, such as infections, chemical injuries, auto-immunitive inflammation, and congenital diseases, which are often associated with corneal angiogenesis [17]. Corneal angiogenesis leads to further scarring and subsequently results in the loss of corneal transparency [18]. However, mechanisms underlying corneal opacity remain largely unknown. Moreover, the treatment of corneal neovascularization largely relies on surgical keratoplasty (corneal transplantation), and non-surgical treatment methods for corneal neovessel formation are still lacking. In addition, patients with severely-formed neovessels are at high risk of graft rejection [19]. Thus, there is a need to identify the primary regulatory molecules that control corneal angiogenesis.

In the connected former study, the *Dscr-1* null mutation introduced to atherosclerotic *ApoE* $^{-/-}$ mice was found to elicit a high-cholesterol lipid profile with increased very low density lipoprotein (VLDL) and LDL levels and decreased high density lipoprotein (HDL) levels. Such a pathological metabolic condition leads to lipid accumulation in the peripheral tissues. In the present study, we show here, loss of *Dscr-1* promoted a pro-inflammatory and pro-angiogenic environment in the cornea. Inflamed corneas in *Dscr-1*$^{-/-}$ mice showed a high degree of infiltration by vascular and lymphatic endothelial cells from the corneal limbus. Global transcriptome analysis revealed that the SDF-1-CXCR4 signaling axis is stimulated by and is highly associated with pathological corneal opacity. Blockage of SDF-1 by neutralizing antibodies significantly abrogated corneal pathological angiogenesis and corneal opacity. Our findings identify the SDF-1-CXCR4 signaling axis as a novel pathological signaling target and demonstrate the role of VEGF-NFAT-mediated angiogenesis in vascular diseases with hypercholesterolemia.

Materials and Methods

The authors declare that all supporting data are available within the article and in the online-only Data Supplement.

Mice

WT C57BL/6j mice were purchased from Clea Japan. *Dscr-1*$^{-/-}$ and *ApoE*$^{-/-}$ mice on C57BL/6j backgrounds have been previously described [12, 20]. All animal care and the experimental procedures were followed by the instruction from the committee with both University of Tokyo (approval number: RAC07105) and Kumamoto University (approval number: 097). All animals were allowed free access to water and diets. Mice were fed a normal laboratory diet (CE-2; CLEA Japan) or a high-fat diet (HFD) (ORIENTAL YEAST) containing 35% fat, 30% maltose, 22% casein, 7% dextrin, and 3.5% minerals. Detailed ingredient is indicated in the manufacturer web site of CLEA Japan and ORIENTAL YEAST. Littermate mice were fed a HFD for 12 weeks from 8-week-old. Only male mice were studied.

Cell Lines

Human embryonic kidney HEK293 cell lines were purchased from the American Type Culture Collection (Manassas, VA). Cells were maintained in Dulbecco's modified Eagle's medium (DMEM) (Sigma-Aldrich), supplemented with 10% feral bovine serum (FBS) (ThermoFisher) at 37 °C in a 5% CO_2 atmosphere in a humidified incubator. Human umbilical vein endothelial cell (HUVEC) and human microvascular endothelial cell (HMVEC) were purchased from LONZA, and maintained in EGM-2 MV growth medium (LONZA) at 37 °C in a 5% CO_2 atmosphere in a humidified incubator.

Induction of Corneal Inflammatory Angiogenesis and Lymphangiogenesis

Corneal neovascularization in 20- to 24-weeks-old male mice by nylon suturing under microscopy was performed according to the previous study [21]. Under general anesthesia, 10-0 nylon suture was placed intra-stromally 1 mm away from the limbal vessel. Ofloxacin ophthalmic ointment was instilled immediately after suturing. For SDF1 neutralizing experiment, sterilized phosphate buffer saline as control or anti-SDF1 antibody (R&D systems) was administered by subconjunctival injection with 200μg/5μl/eye. Cornea and conjunctiva tissues were excised 5 days after sutured and antibody treatment, and double stained with anti-CD31 (BD Biosciences) and anti-LYVE-1 antibodies (Abcam).

Staining and Quantification of Sutured Corneas and HMVEC

X-gal staining of whole sutured cornea was performed according to previous described protocol [13]. Angiogenesis and lymphangiogenesis were quantified as described previously using double staining with CD31/LYVE-1 [21]. Briefly, the excised corneas following neovascularization were rinsed in PBS, and fixed in acetone for 10 min at −20 °C. Subsequently, the corneas were washed thrice in PBS, blocked with 3% BSA in PBS for 48 h at room temperature, stained with rabbit anti-mouse LYVE-1 antibody (Abcam) and rat anti-mouse CD31 antibody (BD Biosciences), and incubated at 4°C overnight. For Sdf-1 and Cxcr4 detection, corneas were stained with rabbit anti-mouse Sdf-1 antibody (Abcam) and

goat anti-mouse Cxcr4 antibody (Abcam). The corneas were washed again with PBS and stained with secondary antibodies for 3 h at room temperature. Double stained whole mounts were analyzed using a fluorescence microscope (BZ-9000; Keyence). The area covered with blood or lymphatic vessels positive for CD31 or LYVE-1 was quantified using *Image J* software. Corneal tissues from human patients of Stevens-Johnson syndrome and fusarium keratomycosis were obtained during penetrating keratoplasty at the Department of Ophthalmology, the University of Tokyo Hospital. Tissues were embedded in paraffin after fixed in 4% paraformaldehyde, and subjected to Hematoxylin-Eosin (HE) or immunohistochemistry of anti-DSCR-1 antibody. This study was approved by the research ethics committee of the Graduate School of Medicine and Faculty of Medicine at the University of Tokyo (G10149) and all procedures conducted in this study adhered to the tenets of the Declaration of Helsinki.

In case of cultured cells, oxLDL-stimulated cells were fixed by 4% paraformaldehyde and ice-cold methanol, and immunostained with mouse anti-human NFAT1 antibody (BD Bioscience). Cells were washed by PBS containing 0.1% Triton-A100 and incubated with goat anti-mouse IgG antibody conjugated AlexaFluor488 (ThermoFisher) counterstained with DAPI for nucleus visualization. Five representative images per sample were randomly captured by fluorescent confocal microscope and determined NFAT1 nuclear-localized levels.

Quantification of VEGF and oxLDL Treatment

Macrophages from mouse were obtained by washing peritoneal cavity with sterilized PBS following the injection of 2 ml thioglycollate broth (BD Bioscience) for 4 days. Endothelial cells were isolated from mouse lung by using DynaBeads (ThermoFisher) conjugated with rat anti-mouse CD31 antibody. Red blood cells were hemolyzed by ACK lysing buffer (ThermoFisher) and number of cells was determined by cell counting. 5 x 10^5 cells/ml of macrophages or endothelial cells were plated and culture overnight. After 16 h starvation with serum-free DMEM, cells were stimulated with 50 μg/ml oxLDL (Alfa Aesar). Supernatant was collected 24 h after stimulation and ELISA (R&D Systems) was performed according to the manufacture's instruction.

Adenovirus-mediated gene expression in HUVEC and HMVEC

The human NFAT were sub-cloned from HUVEC cDNA reverse-transcribed by SuperScript III Reverse Transcriptase with oligo-dT primer (ThermoFisher), and EGFP as control were sub-cloned from pEGP-N1 plasmid (Addgene). To obtain adenovirus carrying NFAT or EGFP, we used pA/CMV/V5-DEST Gateway Vector Kit (Thermo Fisher) according to the manufacture's instruction. For produce and amplify adenovirus, pA/CMV/V5-DEST plasmids were infected to HEK293, and calculated virus titer by Adeno-X Rapid Titer Kit (Takara Bio). Concentrated adenovirus infected with MOI 50 to cultured HUVEC or HMVEC, and samples were incubated for 48 h.

Gene Expression Analysis Using Real-time PCR

Total RNA was extracted from tissues using the RNeasy Micro Kit (Qiagen), converted to cDNA by using the Prime Script reverse transcriptase (Takara-Bio, Shiga, Japan) as per the

manufacturer's instructions, and used for quantitative real-time PCR amplification using SYBR Green (Takara-Bio) with indicated primers (Table I in the online-only Data Supplement).

Measurement of oxidative stress in endothelial cells

Isolation of primary endothelial cells from WT or *Dscr-1*$^{-/-}$ mice lung was performed by DynaBeads system (ThermoFisher). Briefly, whole lung tissue from mice was digested by type II collagenase solution containing DNase I, then lysis red blood cells and determined cell number. Cells were incubated with DynaBeads conjugated with rat anti-mouse CD31 antibody (BD Bioscience) and separated into endothelial and non-endothelial fraction by magnetic separating system. After first isolation, cells were cultured in 20%FBS/DMEM containing non-essential amino acid, sodium pyruvate and antibiotics for five days. For second isolation, expanded cells were harvested and incubated with DynaBeads conjugated with rat anti-mouse CD102 antibody (BD Bioscience) to increase endothelial cell purity. Obtained primary endothelial cells from each mouse were cultured until confluent, and incubated in 0.5%FBS/MCDB131 medium for 18 h starvation. 1μM Cyclosporine (CsA) were treated at 30 min before VEGF stimulation. After 24 h stimulation of VEGF (50ng/ml) or PBS as control, cells were collected and performed TBARS assay (Cell Biolabs) to measure malondialdehyde (MDA) according to manufacturer's instruction. Produced MDA level by oxidative stress were determined at 540nm excitation/590nm emission for fluorometric measurement and quantified concentration of MDA with standard curve.

Expression Array Analysis

Affymetrix GeneChip Mouse Genome 430 2.0 Array (Affymetrix) was utilized for genome-wide transcription analysis. Data were collected and analyzed by GeneChip Scanner 3000 (Affymetrix), and the GeneChip data were analyzed using the Affymetrix GeneChip Operating Software v1.3 by MAS5 algorithms, to obtain signal value (Genechip score) for each probe-set. The average signal in an array was set as cut-off 100 single intensity. Expression array data is available at GEO datasets (GSE130040), analyzed using the GeneSpring GX software (Tomy Digital Biology).

VEGF promoter luciferase assay

Human VEGF promoter (2043bp: from −2046 to −3) was sub-cloned from HUVEC genome and constructed into pGL4.10 luciferase plasmid (Promega). HEK293 cells were co-transfected both pGL4.10-hVEGF-promoter and pRL-SV40 Renilla plasmid as internal control. 1 day later, cells were starved in 0.5%FBS/MCDB131 medium for 18 h, treated with adenovirus carrying EGFP as control or constitutive active form of human NFAT1, and cultured for 24 h. Luciferase reporter assay was performed by Dual-Luciferase Reporter Assay System (Promega) according to manufacturer's procedure. Determination of promoter activity was calculated by following formula as firefly/ renilla luminescence.

Statistical analysis

Data were analyzed by using GraphPad Prism 8.0 (GraphPad Software). The normality and variances of data were tested by appropriate tests such as Kolmogorov-Smirnov test and *F*

test, and shown as the mean ± standard deviation. All data passed normality and equal variance tests. *P* value between two groups was calculated by using standard two-tailed Student's *t*-test. Statistical significance between multiple samples was determined by one- or two-way ANOVA to reveal comparable variance, and each comparison performed by Tukey HSD post-hoc test (Tomy Digital Biology). $P < 0.05$ was considered as significant for most experiments. FDR $q < 0.25$ was considered as significant for GSEA analysis.

Results

Dscr-1$^{-/-}$ and *ApoE*$^{-/-}$ mice spontaneously develop corneal opacity with increasing age

We have shown the hypercholesterolemia metabolic dysfunction is occurred by the ApoE deficiency, which is exaggerated by the combined loss of Dscr-1. To extend the study of these pathology, we continued phenotype analysis and found that corneal opacity was the most prominent feature of *Dscr-1*$^{-/-}$ plus *ApoE*$^{-/-}$ mice even when mice were subjected to normal chow feeding conditions (Figure 1A). To determine the frequency and the severity of corneal opacity, similar aged *Dscr-1* or *ApoE* single null mutant, double null mutant, and littermate WT control mice were studied in parallel. Corneal opacity scores were obtained through macroscopic observation of double knockout mice (Figure 1B, and Figure I in the online-only Data Supplement). Results showed that neither *Dscr-1*$^{-/-}$, *ApoE*$^{-/-}$, nor *Dscr-1*$^{-/-}$ plus *ApoE*$^{-/-}$ double null mutant mice developed abnormal corneal phenotypes at four weeks of age. However, after a latency period of 12 weeks, *Dscr-1*$^{-/-}$ mice gradually developed spontaneous corneal opacity with massive neovascularization and extensive infiltration of inflammatory cells. At 48 weeks, approximately 70% of *Dscr-1*$^{-/-}$ mice developed abnormal corneal phenotypes (Figure 1C and Supplementary Table 1 in the online-only Data Supplement). Remarkably, *Dscr*1$^{-/-}$ and *ApoE*$^{-/-}$ double knockout mice developed severe corneal phenotypes as early as eight weeks of age (Figure 1C). Next, we performed histological examination of the cornea in each mouse. As shown in Figure 1D, loss of Dscr-1 increased infiltration by CD11b-positive leukocytes in the cornea with an even greater increase of leukocyte infiltration in *Dscr-1* and *ApoE* double null mutants. Increased leukocyte infiltration also resulted in corneal angiogenesis (Figure 1D and E). Double null mutant mice exhibited extensive thickening and pathological keratinization of the corneal epithelium with inflammation of the underlying corneal stroma (Figure 1D). Characterization of the corneas in *Dscr-1*$^{-/-}$ and *ApoE*$^{-/-}$ 12-month-old mice showed pronounced recruitment of CD31-positive blood vessels in the cornea concomitant with lipid deposition, which was almost completely absent in WT mice. This implies that the loss of *Dscr-1* leads to extensive infiltration by inflammatory cells. The degree of opacity was also more pronounced in mice with the *ApoE* null mutation.

Dscr-1$^{-/-}$ mice show increased angiogenesis and lymphangiogenesis in a sutured neovascularization model

DSCR-1 expression levels have been shown to be exclusively regulated by NFAT transcription [7, 11]. To test whether the corneal suture model [16] enhances NFAT signaling, DSCR-1 reporter mice were used. Sutured regions in the cornea showed selective upregulation of *lacZ* (Figure 2A), suggesting that corneal opacity is triggered by trauma such as suturing in the cornea, which markedly upregulates NFAT/DSCR-1 signaling in

neovessels. Additionally, to investigate the functional role of *Dscr-1* in inflammatory corneal neovascularization, angiogenic and lymphangiogenic responses of *Dscr-1*$^{-/-}$ mice were compared to those of WT mice in a suture-induced corneal neovascularization model. At 5 days after suturing, there were significantly more vascularized field in the corneas of *Dscr-1*$^{-/-}$ mice as compared to WT mice (Figure 2B). Moreover, immunostainings revealed that CD31-positive vascular endothelial cells and LYVE-1-positive lymphatic vessel endothelial cells in the corneas of *Dscr-1*$^{-/-}$ mice were significantly increased when they were compared to WT mice (Figure 2C–E). While, at day 7 after the suture resulted in the over-calculation window, due to reached to plateau, since *Dscr-1*$^{-/-}$ caused the hyper-angiogenic condition.

Endothelium-selective *Dscr-1* overexpression inhibits corneal neovascularization

NFAT/DSCR-1 signaling and vascular activation exhibit a bell-shaped correlation, implying that DSCR-1 overexpression interferes with neovessel formation [13]. Thus, we performed corneal sutures in DSCR-1 transgenic mice (DSCR-1 Tg) with *DSCR-1* expression driven by the Tie2 promoter leading to stable DSCR-1 expression. In contrast to the lacking of *Dscr-1*, Dscr-1 stable expressions never led to neovascularization on microscopy within the 5 days after the suture experiments. Day 5 after the suture from WT controls failed to reach the effective calculation window. Therefore, we performed day 7 after the suture in comparison between DSCR-1 Tg and WT. As shown in Figure 2F, angiogenesis in the limbus was significantly lower compared to those of WT mice. In particular, immunohistochemical staining using anti-CD31 and anti-LYVE-1 antibodies revealed that suturing triggered pathological angiogenesis in WT mice that was significantly attenuated in *Dscr-1* Tg mice (Figure 2G–I). Compared to WT, CD31-and LYVE1-positive areas were increased in *Dscr-1*$^{-/-}$ at the day 5, whereas reduced in DSCR-1 Tg at the day 7 after the suture experiment (compared through Figure 2 B–I). Taken together, these data suggest that angiogenic and inflammatory stimuli, such as corneal suturing, activates the NFAT/DSCR-1 signaling axis. Endothelial cell-selective overexpression of DSCR-1 blocks neovessel formation, whereas loss of *Dscr-1* promotes pathological angiogenesis and lymphangiogenesis in the limbus. Normal corneas maintain transparency to prevent angiogenesis. Thus, blocking NFAT activation would be a key point for the maintenance of avascularity in cornea.

Dscr-1$^{-/-}$ upregulates pro-angiogenic *Sdf-1*/ *Cxcr4* signaling axis in cornea

To elucidate the molecular mechanisms behind corneal angiogenesis in *Dscr-1*$^{-/-}$ mice, we performed microarray analysis on isolated corneas. A total of 2,083 *Dscr-1* regulated genes were found to be upregulated in the corneas of *Dscr-1*$^{-/-}$ mice compared to WT mice. Many of them were belong to immune-system related genes from GO analysis (Figure 3A and B). More importantly, we focused the gene set that suture mediated further induced by Dscr-1 null mutation, but reduced by DSCR-1 Tg. Totally 126 gene set were categorized them, which was predominantly related cell migration and angiogenesis (Figure 3A and B). Angiogenesis and cell migration are tightly correlated corneal opacity, thus the categorized 126 genes were selected for further analysis. The heat map in Figure 3B shows the expression profiles of pro-angiogenic genes, including *Sdf-1*, *Apj*, and *Plvap* whose increased expression was further confirmed by real-time qRT-PCR (Figure 3C and Figure

IIA in the online-only Data Supplement). Importantly, *Dscr-1*$^{-/-}$-mediated induced genes were similarly downregulated in the cornea samples from DSCR-1 transgenic mice. In contrast, gene expression that was reduced in *Dscr-1*$^{-/-}$ condition such as *Serum amyloid A1* and *Dermokine* are known to have anti-angiogenic properties [22, 23] and were similarly induced in DSCR-1 transgenic mice (Figure IIB in the online-only Data Supplement). SDF-1 and its receptor system; CXCR4/7, represents a crucial angiogenic pathway in developmental as well as pathological processes. Moreover, it has been reported that SDF-1/CXCR4 signaling and CXCR4 expression in lymphatic endothelium regulates lymphatic network formation [24], and tumor lymphangiogenesis [25]. Interestingly, loss of *Dscr-1* stimulates not only CXCR7 induction during the acute phase [26], but also promotes CXCR4 expression in angiogenic microvascular endothelial cells (Figure 3D and E). DSCR-1 transgenic mice in turn downregulated CXCR4 expression (Figure 3F). Immunohistochemistry and semi-quantification of SDF-1 and CXCR4 expression in sutured cornea showed significant upregulation of these protein in *Dscr-1*$^{-/-}$mice that were significantly reduced in DSCR-1 transgenic mice (Figure 4A to D). Of note, besides Sdf-1-Cxcr4 axis, Apj-Apelin pro-angiogenic axis was also upregulated in cornea of *Dscr-1*$^{-/-}$mice (Figure III in the online-only Data Supplement). Taken together, loss of DSCR-1 promotes *Sdf-1* and *Cxcr4* expression in the corneal microenvironment leads to angiogenesis into avascular regions.

Hypercholesterolemia-mediated oxLDL treatment promotes the angiogenic switch in *Dscr-1*$^{-/-}$ endothelial cells

Corneal opacities were more pronounced in *Dscr-1*$^{-/-}$ mice on an *ApoE*$^{-/-}$ background. Loss of APOE caused hypercholesterolemia with increased peripheral circulation of denatured LDL [20]. Various pathological phenotypes of *ApoE*$^{-/-}$ mice have been previously reported; however, most studies were based upon atherosclerotic progression mediated by increased LDL and reduced HDL circulation during the chronic phase [27] with this phenotype observed only in older mice. We hypothesized that the accumulation of oxidative stresses in aged mice increases corneal opacity (Figure 1C) and that *ApoE*$^{-/-}$-mediated increases in oxLDL levels leads to severe corneal opacity. VEGF is the most well-known endothelial cell activator and plays a primary role in the calcineurin-NFAT pathway. *Dscr-1* null mutations resulted in NFAT hyper-activation [11, 12] and increased the susceptibility of oxidation [28].To that end, we first subjected lipid peroxidation assay with malondialdehyde (MDA) to quantify the oxidative stress. As shown in Figure 5A, compared to littermate WT controls, Dscr-1 null mutation hyper-induced oxidative stress which was markedly mitigated by the calcineurin-NFAT inhibitor, cyclosporine A (CsA). Thus, increased LDL due to loss of *ApoE* is susceptible to oxidation. Moreover, upregulated oxLDL directly activated NFAT nuclear localization in microvascular endothelial cells (Figure 5B). OxLDL treatment led to a 3.3-fold increase in *Sdf-1* expression comparable to *Vcam-1*, a well-known response to oxLDL in endothelial cells [29](Figure 5C). OxLDL also influenced macrophage activation. It is known that macrophage infiltration in inflamed tissue express high levels of VEGF [30]. Additionally, autocrine expression of VEGF from endothelial cells also play an important role. Levels of secreted VEGF from macrophages were significantly higher in the presence of oxLDL, which were larger than from endothelium (Figure 5D). NFAT was a key transcriptional regulator of VEGF gene expression (Figure 5E). Interestingly, VEGF levels

were 2.2-fold higher in *Dscr-1*$^{-/-}$ mice than in WT mice in the absence of oxLDL. Macrophages of *Dscr-1*$^{-/-}$ mice showed the highest VEGF secretion levels as a result of oxLDL treatment (Figure 5D). Consistent with these results, NFAT activation and oxidative stimuli resulted in the upregulation of both SDF-1 and its receptor, CXCR4, in HMVEC (Figure 5F). Taken together, these data suggest that *ApoE*$^{-/-}$- and *Dscr-1*$^{-/-}$-mediated increased peripheral oxLDL level promotes VEGF secretion from infiltrated macrophages in cornea, which in turn further stimulates angiogenesis by inducing the expression of *Sdf-1* and its receptor, *Cxcr4* (Figure 5G).

Anti-SDF-1 attenuates *Dscr-1*$^{-/-}$-induced corneal opacity

Our findings suggest that the SDF-1-CXCR4/7 signaling axis is involved in the pathogenesis of corneal opacity in *Dscr-1*$^{-/-}$ mice. To test whether inhibiting SDF-1 signaling can prevent corneal opacity, we administrated neutralizing antibodies against SDF-1 in the cornea. *Dscr-1* null mice showed more than 2-fold higher stimulation of suture-induced infiltration by CD31-positive vascular endothelial cells and LYVE-1-positive lymphatic endothelial cells, compared to WT control. Importantly, anti-SDF-1 antibody administration completely abrogated pathological angiogenesis in the cornea (Figure IV in the online-only Data Supplement). Moreover, to distinguish whether SDF-1 neutralization is also applicable hypercholesterolemia-driven severe corneal opacity, suture assays were performed in corneas of *Dscr-1*$^{-/-}$ and *ApoE*$^{-/-}$ mice. Remarkably, significant corneal angiogenesis and lymphangiogenesis was observed in double knockout mice (Figure 6A), which was attenuated by 85% and 53% upon SDF-1 inhibition, respectively (Figure 6B and C). Thus, early onset corneal opacity mediated by loss of *Dscr-1* and *ApoE* is regulated in part by SDF-1 signaling. SDF-1 blockage represents a potential therapeutic strategy in the treatment of corneal neo-vascularization and subsequent opacity.

DSCR-1 is expressed in human patients of Stevens-Johnson syndrome and fusarium keratomycosis

The VEGF-NFAT/DSCR-1 signaling axis is involved in tumor angiogenesis during solid tumor growth in Down syndrome patients and type II diabetes in human [31, 32]. Moreover, Stevens-Johnson Syndrome and toxic epidermal necrosis are very serious skin conditions that can happen as a result of illness or as a side effect to certain medications. It was previously reported that ocular surface impaired neovascularization in these patients was attenuated by the treatment of anti-VEGF antibody [33]. Moreover, long term tacrolimus treatment was shown to induce anti-angiogenic and anti-inflammatory effects to injured corneas via VEGF-NFAT function [34].To test whether corneal inflammation in humans also activates the NFAT/DSCR-1 axis, we examined DSCR-1 expression via immunohistochemical analysis of corneal samples from patients with Stevens-Johnson syndrome and fusarium keratomycosis. Inflamed corneas revealed advanced angiogenesis as evidenced by a high degree of invasion by CD34-positive vascular endothelial cells (Figure 6D). More importantly, NFAT/DSCR-1 signaling was found to be upregulated in subsets of endothelial cells in the neovessels of inflamed corneas (Figure 6D). These results demonstrate the clinical relevance of NFAT signaling and its involvement in the progression of corneal diseases. Mechanistically, loss or overexpression of DSCR-1 resulted in the

hyper-stimulation or inhibition of VEGF-mediated NFAT signaling and oxidative response, leading that enhanced or attenuated corneal inflammation, respectively.

Discussion

Vascular homeostasis is an indispensable most important system in organisms. Once, the vascular system is broken or dysfunction, which is believed to directly trigger morbidity and mortality. Pathological conditions in larger vessels have been well studied. However, studies on peripheral tissues or the microenvironment in smaller vessels are currently lacking. In the present study, we demonstrated that DSCR-1 null mutant mice spontaneously developed corneal opacity with increasing age and that DSCR-1 is associated with corneal angiogenesis and infiltration by inflammatory cells. This pathology was highly pronounced under $ApoE^{-/-}$-mediated hypercholesterolemia and hyperlipidemia conditions. Corneas of $Dscr\text{-}1^{-/-}$ mice showed increased angiogenesis and lymphangiogenesis in a suture-induced corneal neovascular model, whereas DSCR-1 Tg mice showed markedly dampened pathology in these models.

DSCR-1 (also known as RCAN1, MCIP1, or calcipressin) was named as such because it is located in the Down syndrome critical region of human chromosome 21 [35]. We and others have identified that VEGF or thrombin dramatically and rapidly upregulated DSCR-1 via NFAT and GATA binding on the regulatory region, which in turn adequately modulates calcineurin-NFAT signaling both in primary cultured endothelial cells and *in vivo* [7, 10, 11, 36]. Overexpression or trisomic expression of DSCR-1 attenuates calcineurin-NFAT signaling, which elicits anti-inflammatory and anti-angiogenic responses mainly by attenuating endothelial cell activation. Indeed, DSCR-1 stable expression in mice protects against endotoxemia-induced lethality, solid tumor growth, and metastasis to the lungs [11, 13]. By contrast, loss of DSCR-1 results in NFAT hyperactivation at least in endothelial cells, which presented divergent phenotypes due to the different microenvironments [12]. Well-organized or highly vascularized pre-set organs, such as the lungs, showed increased angiogenesis and enhanced expression of cell adhesion molecules in endothelial cells, which subsequently led to early onset of tumor metastasis under the $Dscr\text{-}1^{-/-}$ condition. Meanwhile, primary solid tumors or organs subjected to acute endotoxemic shocks showed strong expression of VEGF and other inflammatory cytokines, so that that $Dscr\text{-}1^{-/-}$ endothelial cells ‘re-routed’ downstream signaling to apoptotic fates due to the over-threshold of endothelial cell homeostasis. Thus, mice lacking DSCR-1 showed various phenotypes depending on the tissues and organs. The calcineurin-NFAT/DSCR-1 signaling axis plays a crucial role in vascular-bed heterogeneity in whole organs.

Under normal conditions, corneal transparency is maintained due to the surrounding avascular microenvironment. By contrast, in pathological conditions, the angiogenic switch is turned on. In the current study, genome-wide screening was performed to elucidate the molecular mechanisms underlying corneal opacity and to determine DSCR-1 function. Comprehensive data sets revealed that the SDF-1/CXCL12 and its receptor system are associated with corneal opacity. We show that the *Dscr-1* null mutation markedly increased *sdf-1* expression in sutured cornea microenvironment. In the arrays in Figure 3A, Dscr-1 null mice had a large number of changed genes, when compared to littermate WT control. On the

contrary, suture treatment by itself caused marked induction with angiogenic and inflammatory related genes in both WT and Dscr-1 null mice. As a result, a smaller number but important gene sets can be induced in Dscr-1$^{-/-}$ mice compared to those without suture treatment. The *Dscr-1*$^{-/-}$ condition exerts various effects on endothelial cells. Indeed, primary cultured microvascular endothelial cells from *Dscr-1*$^{-/-}$ mice showed increased expression of angiogenic-and inflammatory genes, including *Angiopoietin2* and *Vcam1*. Importantly, SDF-1/CXCR4 autocrine (self-activation via ligand and the receptor) systems were found to be stimulated in *Dscr-1*$^{-/-}$ microvascular endothelial cells in inflamed corneas (Figure 5).

The SDF-1/CXCR4 axis has been well reported as a crucial signaling factor for survival, cell proliferation, migration, and angiogenesis in expressed stem cells, stromal cells, or endothelial cells [9, 26]. Furthermore, there is wide availability of neutralizing antibodies against SDF-1 or chemical antagonists against CXCR4. Importantly, administration of neutralizing antibodies against SDF-1 successfully prevents corneal neovascularization under the *Dscr-1*$^{-/-}$ microenvironment. NFAT is a primary factor affecting DSCR-1 expression in the endothelium. Furthermore, angiogenic endothelial cells in human patients were also observed to exhibit DSCR-1 upregulation in the corneas (Figure 6D). Taken together, these findings suggest that blocking SDF-1/CXCR4 signaling can represent a novel therapeutic strategy against pathological corneal opacity caused by NFAT/DSCR-1 - stimulated inflammation.

Intriguing results from the current study show that *Dscr-1*$^{-/-}$ mice gradually developed corneal opacity with increasing age, and *Dscr-1* and *ApoE* double null mutant mice showed dramatically exaggerated eye pathologies. DSCR-1, originally named as Adapt78, has been reported as an anti-oxidative stress factor [28, 37]. Overexpression of DSCR-1 protects against apoptosis from superoxide treatment [38]. Noteworthy, we first indicated loss of DSCR-1 in turn increased oxidative stress (Figure 5A). *ApoE*$^{-/-}$ mice exhibit increased vLDL and LDL levels and decreased HDL levels, similar to human cholesterol profiles. *ApoE*$^{-/-}$ mice showed upregulation of denatured LDL levels with increasing age [20, 39]. Thus, we hypothesized that the *Dscr-1*$^{-/-}$ condition increases sensitivity to oxidative stimuli and that hypercholesterolemia induced by the *ApoE*$^{-/-}$ mutation causes oxLDL accumulation in the eyes, which in turn stimulates pathological peripheral angiogenesis. Age-dependent oxidation levels in peripheral cornea of mice are difficult to quantify; however, oxLDL treatment was shown to activate NFAT following to upregulate SDF-1 and CXCR4 expressions in microvascular endothelial cells and lead to increased VEGF secretion by inflammatory macrophages. Induction levels were higher in *Dscr-1*$^{-/-}$ mice than WT controls (Figure 5D). Interestingly, the degrees of oxLDL sensitivity and downstream NFAT/DSCR-1 signaling can vary depending on the vascular-bed of the target organ being studied. In contrast to microvascular endothelial cells, endothelial cells derived from large vessels, such as umbilical vein (HUVEC) or aorta, failed to induce Sdf-1 expression under oxLDL treatment [40, 41]. Moreover, NFAT overexpression in HUVEC markedly induced Cxcr4 and Cxcr7 but failed to upregulate Sdf-1 expression. Compared to HUVEC [26], microvascular endothelial cells did not exhibit significant Cxcr7 upregulation upon Ad-NFAT treatment (Figure V in the online-only Data Supplement). Taken together, these data suggest that

ApoE$^{-/-}$-mediated chronic oxLDL stimulation and *Dscr-1*$^{-/-}$-mediated NFAT hyperactivation leads to substantial corneal opacity with increasing age.

In conclusion, DSCR-1 can be a protective factor against chronic corneal neovessel formation, as well as acute septic inflammation. oxLDL stimulates VEGF secretion in pathological corneas, which triggers further angiogenesis via NFAT activation in the corneal endothelium. Results suggest that the NFAT-SDF-1/CXCR4 signaling axis is a key regulator for corneal neovascularization.

Supplementary Material

Refer to Web version on PubMed Central for supplementary material.

Acknowledgements

We thank Ms. Hiroko Meguro and Prof. Hiroyuki Aburatani (RCAST, The University of Tokyo) for technical assistance with microarrays

Sources of funding

This study was supported by a Grant-in-Aid for Scientific Research on Innovative Areas from Ministry of Education, Culture, Spots, Sciences, and Technology in Japan (to TM), and in part by Sankyo science foundation in Japan (to TM).

Nonstandard Abbreviations and Acronyms

VEGF	Vascular endothelial growth factor
NFAT	Nuclear factor for activated T cells
DSCR-1	Down syndrome critical region-1
APOE	Apolipoprotein E
SDF-1	Stromal derived factor-1
WT	Wild-type
oxLDL	oxidized low density lipoprotein
Ad	Adenovirus
MDA	Malondialdehyde
LYVE-1	Lymphatic vessel endothelial hyaluronan receptor-1
Tg	transgenic

References

1. Minami T, Aird WC. Endothelial cell gene regulation. Trends in cardiovascular medicine. 2005;15:174–184 [PubMed: 16165014]
2. Aird WC. Phenotypic heterogeneity of the endothelium: I. Structure, function, and mechanisms. Circulation research. 2007;100:158–173 [PubMed: 17272818]

3. Aird WC. Phenotypic heterogeneity of the endothelium: Ii. Representative vascular beds. Circulation research. 2007;100:174–190 [PubMed: 17272819]
4. Armesilla AL, Lorenzo E, Gomez del Arco P, Martinez-Martinez S, Alfranca A, Redondo JM. Vascular endothelial growth factor activates nuclear factor of activated t cells in human endothelial cells: A role for tissue factor gene expression. Molecular and cellular biology. 1999;19:2032–2043 [PubMed: 10022890]
5. Lambrechts D, Carmeliet P. Sculpting heart valves with nfatc and vegf. Cell. 2004;118:532–534 [PubMed: 15339657]
6. Hernandez GL, Volpert OV, Iniguez MA, Lorenzo E, Martinez-Martinez S, Grau R, Fresno M, Redondo JM. Selective inhibition of vascular endothelial growth factor-mediated angiogenesis by cyclosporin a: Roles of the nuclear factor of activated t cells and cyclooxygenase 2. The Journal of experimental medicine. 2001;193:607–620 [PubMed: 11238591]
7. Minami T, Horiuchi K, Miura M, Abid MR, Takabe W, Noguchi N, Kohro T, Ge X, Aburatani H, Hamakubo T, Kodama T, Aird WC. Vascular endothelial growth factor- and thrombin-induced termination factor, down syndrome critical region-1, attenuates endothelial cell proliferation and angiogenesis. The Journal of biological chemistry. 2004;279:50537–50554 [PubMed: 15448146]
8. Minami T, Sugiyama A, Wu SQ, Abid R, Kodama T, Aird WC. Thrombin and phenotypic modulation of the endothelium. Arterioscler Thromb Vasc Biol. 2004;24:41–53 [PubMed: 14551154]
9. Mirshahi F, Pourtau J, Li H, Muraine M, Trochon V, Legrand E, Vannier J, Soria J, Vasse M, Soria C. Sdf-1 activity on microvascular endothelial cells: Consequences on angiogenesis in in vitro and in vivo models. Thrombosis research. 2000;99:587–594 [PubMed: 10974345]
10. Hesser BA, Liang XH, Camenisch G, Yang S, Lewin DA, Scheller R, Ferrara N, Gerber HP. Down syndrome critical region protein 1 (dscr1), a novel vegf target gene that regulates expression of inflammatory markers on activated endothelial cells. Blood. 2004;104:149–158 [PubMed: 15016650]
11. Minami T, Yano K, Miura M, Kobayashi M, Suehiro J, Reid PC, Hamakubo T, Ryeom S, Aird WC, Kodama T. The down syndrome critical region gene 1 short variant promoters direct vascular bed-specific gene expression during inflammation in mice. The Journal of clinical investigation. 2009;119:2257–2270 [PubMed: 19620774]
12. Ryeom S, Baek KH, Rioth MJ, Lynch RC, Zaslavsky A, Birsner A, Yoon SS, McKeon F. Targeted deletion of the calcineurin inhibitor dscr1 suppresses tumor growth. Cancer cell. 2008;13:420–431 [PubMed: 18455125]
13. Minami T, Jiang S, Schadler K, Suehiro J, Osawa T, Oike Y, Miura M, Naito M, Kodama T, Ryeom S. The calcineurin-nfat-angiopoietin-2 signaling axis in lung endothelium is critical for the establishment of lung metastases. Cell reports. 2013;4:709–723 [PubMed: 23954784]
14. Zaichuk TA, Shroff EH, Emmanuel R, Filleur S, Nelius T, Volpert OV. Nuclear factor of activated t cells balances angiogenesis activation and inhibition. The Journal of experimental medicine. 2004;199:1513–1522 [PubMed: 15184502]
15. Corrent G, Roussel TJ, Tseng SC, Watson BD. Promotion of graft survival by photothrombotic occlusion of corneal neovascularization. Archives of ophthalmology. 1989;107:1501–1506 [PubMed: 2478111]
16. Zhu SN, Dana MR. Expression of cell adhesion molecules on limbal and neovascular endothelium in corneal inflammatory neovascularization. Investigative ophthalmology & visual science. 1999;40:1427–1434 [PubMed: 10359324]
17. Abdelfattah NS, Amgad M, Zayed AA, Hussein H, Abd El-Baky N. Molecular underpinnings of corneal angiogenesis: Advances over the past decade. International journal of ophthalmology. 2016;9:768–779 [PubMed: 27275438]
18. Sankar MJ, Sankar J, Mehta M, Bhat V, Srinivasan R. Anti-vascular endothelial growth factor (vegf) drugs for treatment of retinopathy of prematurity. The Cochrane database of systematic reviews. 2016;2:CD009734
19. Bachmann B, Taylor RS, Cursiefen C. Corneal neovascularization as a risk factor for graft failure and rejection after keratoplasty: An evidence-based meta-analysis. Ophthalmology. 2010;117:1300–1305 e1307 [PubMed: 20605214]

20. Maor I, Hayek T, Coleman R, Aviram M. Plasma ldl oxidation leads to its aggregation in the atherosclerotic apolipoprotein e-deficient mice. Arteriosclerosis, thrombosis, and vascular biology. 1997;17:2995–3005
21. Toyono T, Usui T, Yokoo S, Kimakura M, Nakagawa S, Yamagami S, Miyata K, Oike Y, Amano S. Angiopoietin-like protein 2 is a potent hemangiogenic and lymphangiogenic factor in corneal inflammation. Investigative ophthalmology & visual science. 2013;54:4278–4285 [PubMed: 23702783]
22. Lung HL, Man OY, Yeung MC, et al. Saa1 polymorphisms are associated with variation in antiangiogenic and tumor-suppressive activities in nasopharyngeal carcinoma. Oncogene. 2015;34:878–889 [PubMed: 24608426]
23. Hasegawa M, Higashi K, Matsushita T, Hamaguchi Y, Saito K, Fujimoto M, Takehara K. Dermokine inhibits elr(+)cxc chemokine expression and delays early skin wound healing. J Dermatol Sci. 2013;70:34–41 [PubMed: 23428944]
24. Cha YR, Fujita M, Butler M, Isogai S, Kochhan E, Siekmann AF, Weinstein BM. Chemokine signaling directs trunk lymphatic network formation along the preexisting blood vasculature. Developmental cell. 2012;22:824–836 [PubMed: 22516200]
25. Zhuo W, Jia L, Song N, Lu XA, Ding Y, Wang X, Song X, Fu Y, Luo Y. The cxcl12-cxcr4 chemokine pathway: A novel axis regulates lymphangiogenesis. Clin Cancer Res. 2012;18:5387–5398 [PubMed: 22932666]
26. Suehiro J, Kanki Y, Makihara C, Schadler K, Miura M, Manabe Y, Aburatani H, Kodama T, Minami T. Genome-wide approaches reveal functional vascular endothelial growth factor (vegf)-inducible nuclear factor of activated t cells (nfat) c1 binding to angiogenesis-related genes in the endothelium. The Journal of biological chemistry. 2014;289:29044–29059 [PubMed: 25157100]
27. Chen Z, Ishibashi S, Perrey S, et al. Troglitazone inhibits atherosclerosis in apolipoprotein e-knockout mice: Pleiotropic effects on cd36 expression and hdl. Arteriosclerosis, thrombosis, and vascular biology. 2001;21:372–377
28. Ermak G, Harris CD, Davies KJ. The dscr1 (adapt78) isoform 1 protein calcipressin 1 inhibits calcineurin and protects against acute calcium-mediated stress damage, including transient oxidative stress. FASEB journal : official publication of the Federation of American Societies for Experimental Biology. 2002;16:814–824 [PubMed: 12039863]
29. Kita T, Kume N, Minami M, Hayashida K, Murayama T, Sano H, Moriwaki H, Kataoka H, Nishi E, Horiuchi H, Arai H, Yokode M. Role of oxidized ldl in atherosclerosis. Annals of the New York Academy of Sciences. 2001;947:199–205; discussion 205-196 [PubMed: 11795267]
30. Ramos MA, Kuzuya M, Esaki T, Miura S, Satake S, Asai T, Kanda S, Hayashi T, Iguchi A. Induction of macrophage vegf in response to oxidized ldl and vegf accumulation in human atherosclerotic lesions. Arteriosclerosis, thrombosis, and vascular biology. 1998;18:1188–1196
31. Baek KH, Zaslavsky A, Lynch RC, et al. Down's syndrome suppression of tumour growth and the role of the calcineurin inhibitor dscr1. Nature. 2009;459:1126–1130 [PubMed: 19458618]
32. Peiris H, Duffield MD, Fadista J, et al. A syntenic cross species aneuploidy genetic screen links rcan1 expression to beta-cell mitochondrial dysfunction in type 2 diabetes. PLoS genetics. 2016;12:e1006033 [PubMed: 27195491]
33. Uy HS, Chan PS, Ang RE. Topical bevacizumab and ocular surface neovascularization in patients with stevens-johnson syndrome. Cornea. 2008;27:70–73 [PubMed: 18245970]
34. Chen L, Zhong J, Li S, Li W, Wang B, Deng Y, Yuan J. The long-term effect of tacrolimus on alkali burn-induced corneal neovascularization and inflammation surpasses that of anti-vascular endothelial growth factor. Drug Des Devel Ther. 2018;12:2959–2969
35. Fuentes JJ, Pritchard MA, Estivill X. Genomic organization, alternative splicing, and expression patterns of the dscr1 (down syndrome candidate region 1) gene. Genomics. 1997;44:358–361 [PubMed: 9325060]
36. Minami T, Miura M, Aird WC, Kodama T. Thrombin-induced autoinhibitory factor, down syndrome critical region-1, attenuates nfat-dependent vascular cell adhesion molecule-1 expression and inflammation in the endothelium. The Journal of biological chemistry. 2006;281:20503–20520 [PubMed: 16627481]

37. Leahy KP, Crawford DR. Adapt78 protects cells against stress damage and suppresses cell growth. Archives of biochemistry and biophysics. 2000;379:221–228 [PubMed: 10898938]

38. Ermak G, Cheadle C, Becker KG, Harris CD, Davies KJ. Dscr1(adapt78) modulates expression of sod1. FASEB J. 2004;18:62–69 [PubMed: 14718387]

39. Liu M, Zhang W, Li X, Han J, Chen Y, Duan Y. Impact of age and sex on the development of atherosclerosis and expression of the related genes in apoe deficient mice. Biochem Biophys Res Commun. 2016;469:456–462 [PubMed: 26592663]

40. Jin F, Hagemann N, Schafer ST, Brockmeier U, Zechariah A, Hermann DM. Sdf-1 restores angiogenesis synergistically with vegf upon ldl exposure despite cxcr4 internalization and degradation. Cardiovascular research. 2013;100:481–491 [PubMed: 24014104]

41. Deng DX, Tsalenko A, Vailaya A, Ben-Dor A, Kundu R, Estay I, Tabibiazar R, Kincaid R, Yakhini Z, Bruhn L, Quertermous T. Differences in vascular bed disease susceptibility reflect differences in gene expression response to atherogenic stimuli. Circulation research. 2006;98:200–208 [PubMed: 16373601]

Highlights

- Loss of Dscr-1 in ApoE$^{-/-}$ mouse dramatically increases corneal opacity with age.
- Deficiency of both *Dscr-1* and *ApoE* induces abnormal angiogenesis, lymphangiogenesis and leukocyte infiltration into cornea.
- NFAT-DSCR-1 signal mediates corneal neovascularization and lymphangiogenesis by activating pro-angiogenic pathway, SDF-1-CXCR4 axis.
- Hyper-oxidative stress from Dscr-1$^{-/-}$ elevated oxLDL in ApoE$^{-/-}$-mediated hypercholesterolemia, that enhances not only SDF-1-CXCR4 axis in microvascular endothelial cells but also secretion of VEGF from inflamed macrophages.
- Neutralization of SDF-1 inhibits pathological corneal neovascularization and lymphangiogenesis.

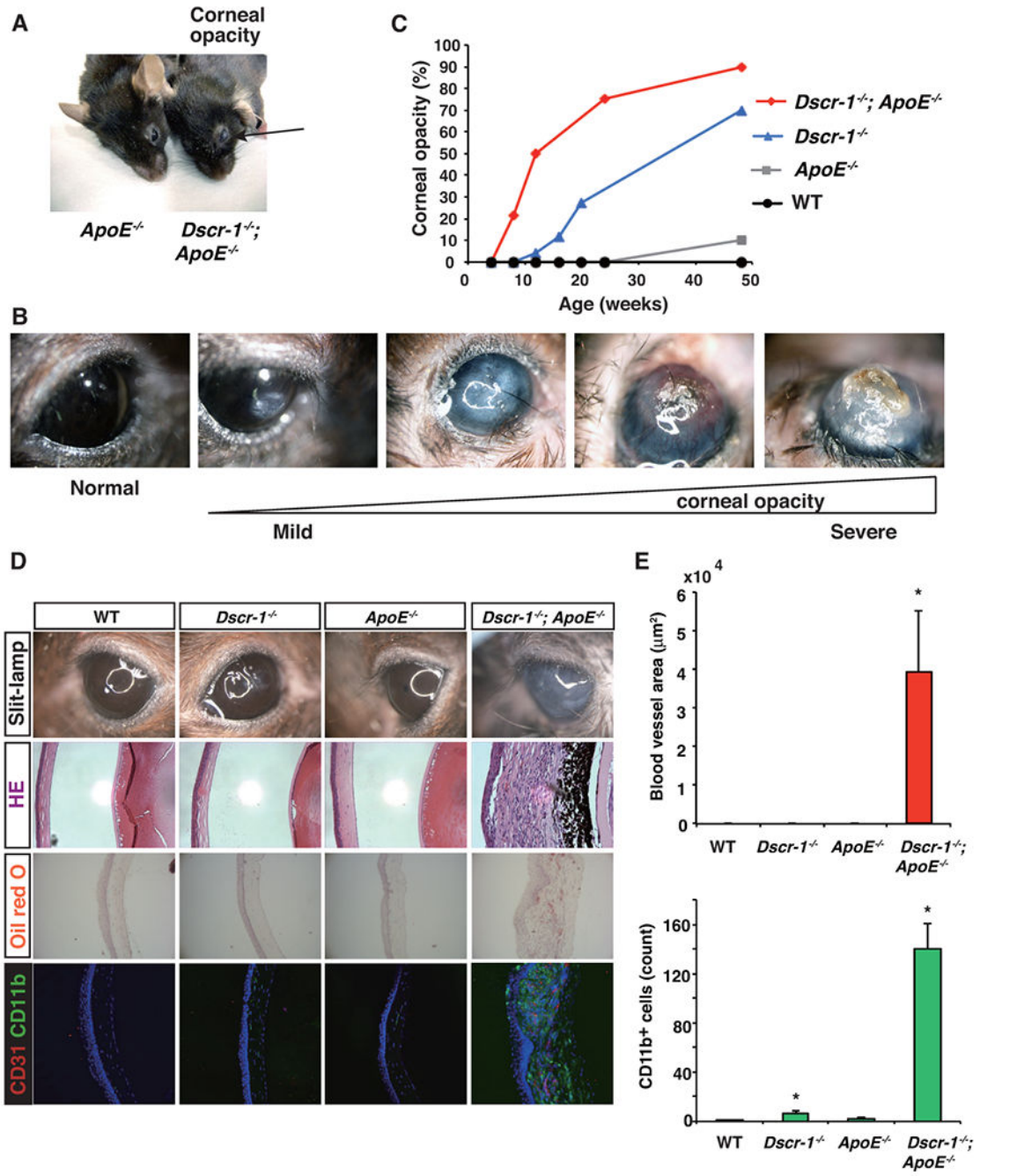

Figure 1. The development of corneal opacity in *Dscr-1* and *ApoE* double knockout mice associated with corneal angiogenesis.

(**A**) Representative 3 month old mice pathology, *ApoE* null; *left*, and *Dscr-1* & *ApoE* double null mouse; *right*. Arrow indicated corneal opacity. (**B**) Representative corneal photographs of mild to severe opacity. (**C**) Percentage of aged mouse eyes with corneal opacity under natural observation (n = 20). (**D**) Representative slit-lamp photograph, HE staining, oil-red O staining and immunostaining of $CD31^+$ blood vessel and $CD11b^+$ macrophages of cornea in 3 month old WT, *Dscr-1*$^{-/-}$, *ApoE*$^{-/-}$, and *Dscr-1* and *ApoE* double knockout mice

(*Dscr-1*$^{-/-}$ & *ApoE*$^{-/-}$). (**E**) Quantification of CD31^{+} blood vessel area (μm^{2}) and CD11b^{+} cells (counts) in WT, *Dscr-1*$^{-/-}$, *ApoE*$^{-/-}$ and *Dscr-1*$^{-/-}$& *ApoE*$^{-/-}$ mice. The mean and ± SD were derived from three independent specimens. *, P<0.05 compared with WT.

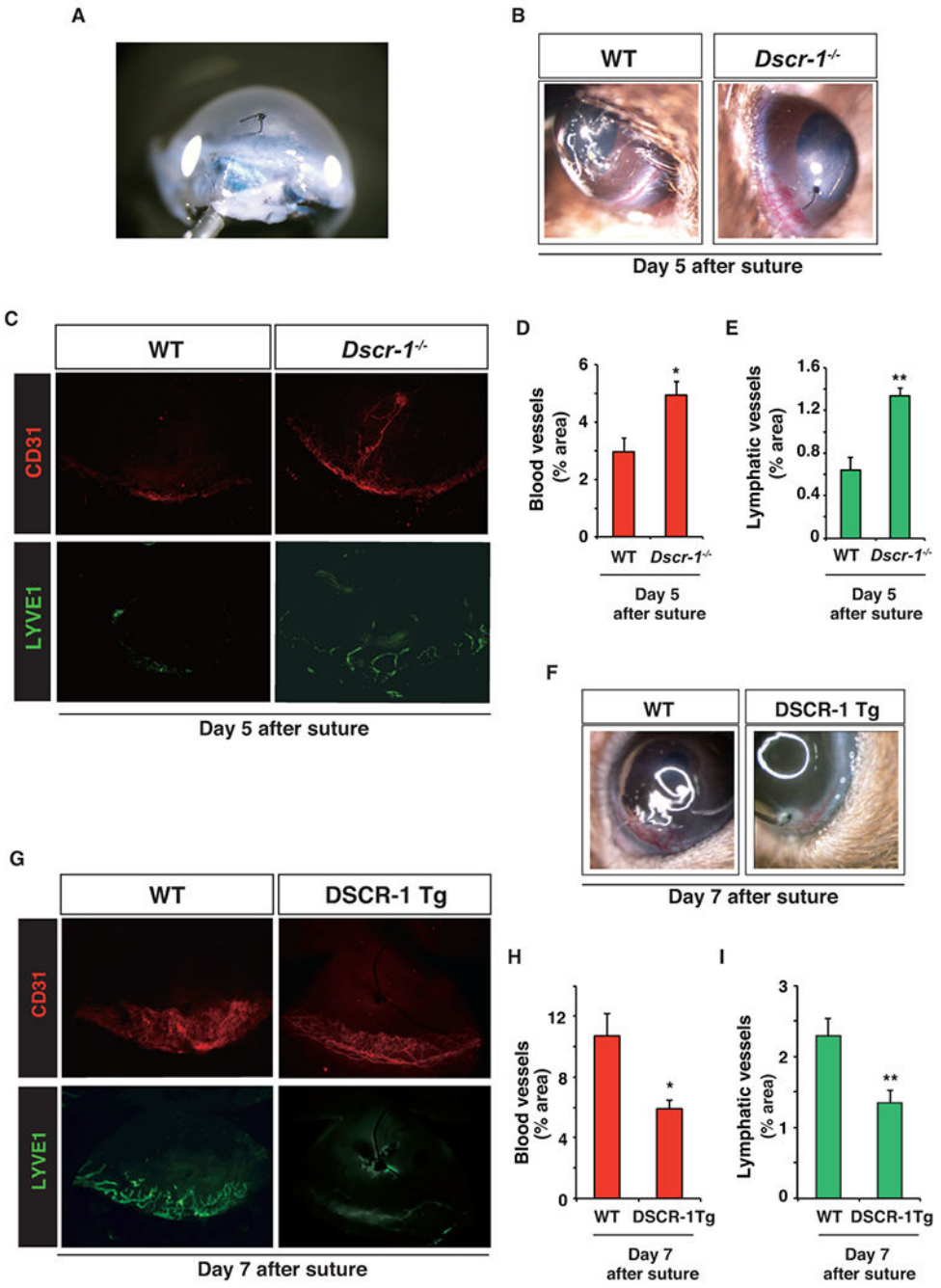

Figure 2. Dscr-1 expression level reflected the corneal angiogenesis and lymphangiogenesis activities in intrastromal sutured cornea.

(**A**) Representative slit-lamp photographs for DSCR-1 promoter mediated *lac*Z expression of mice corneas on day 7 after the intrastromal suturing with 10-0 nylon. (**B**) Representative slit-lamp photographs for WT or *Dscr-1* knockout mice corneas on day 5 after the intrastromal suturing. (**C**) Representative CD31-positive angiogenic or Lyve1-positive lymphangiogenic responses of mice corneas on day 5 after the intrastromal suturing. (**D** and **E**) Surface areas of corneal angiogenesis (*D*) and lymphangiogenesis (*E*) were quantified

with vascularized area versus total corneal area. The mean ± SD were derived from six independent mice. *, P<0.04 compared with WT, and **, P<0.004 compared with WT. (**F**) Representative slit-lamp photographs for WT or DSCR-1 Tg mice corneas on day 7 after the intrastromal suturing. (**G**) Representative CD31-positive angiogenic or Lyve1-positive lymphangiogenic responses of mice corneas on day 7 after the intrastromal suturing. (**H** and **I**) Surface areas of corneal angiogenesis (*H*) and lymphangiogenesis (*I*) were quantified with vascularized area versus total corneal area. The mean ± SD were derived from five independent mice. *, P<0.02 and **, P<0.05 compared with WT.

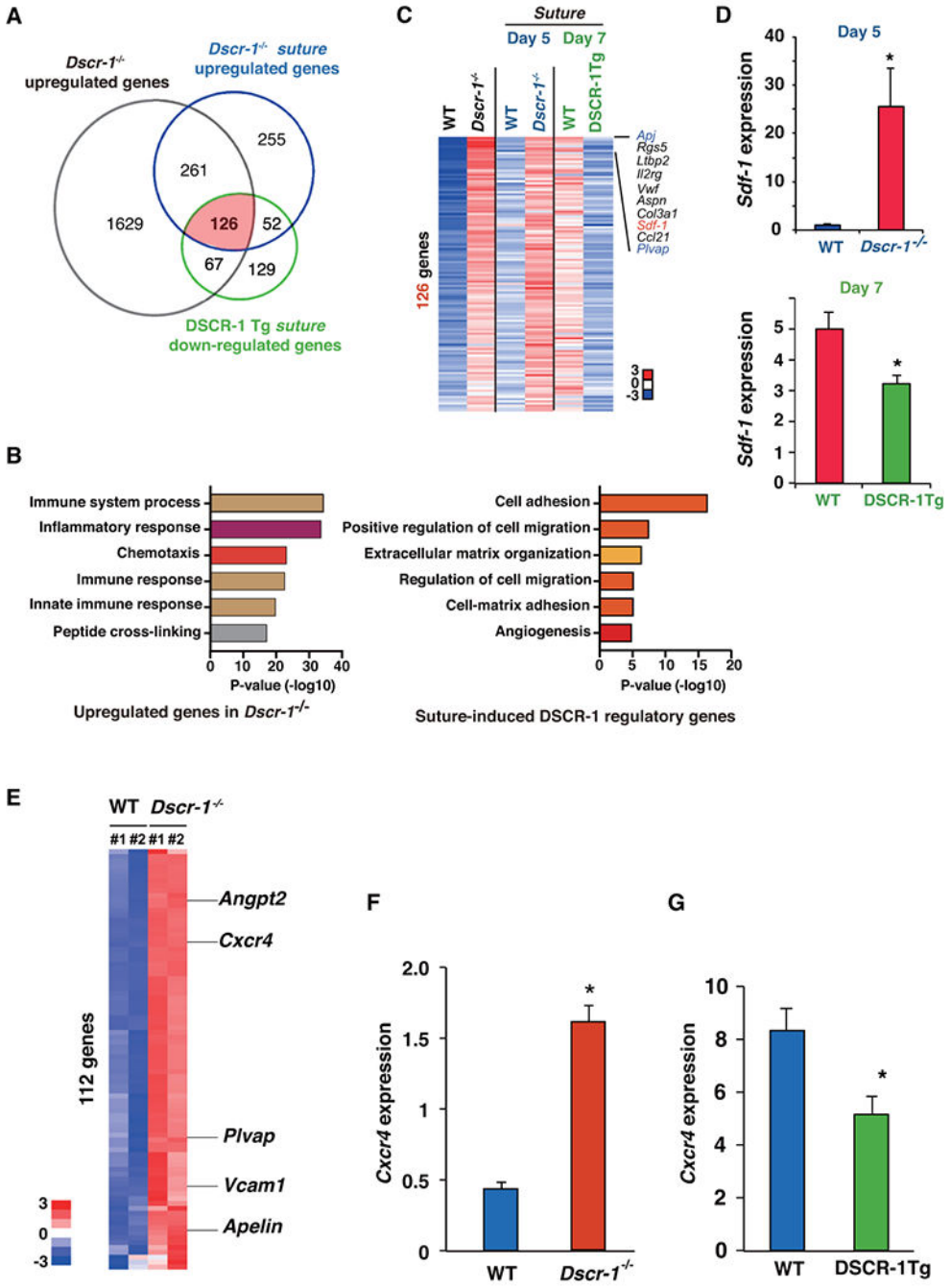

Figure 3. *Dscr-1*$^{-/-}$ increased expression of pro-angiogenic *genes* in cornea.

(**A**) Venn diagram representation of the genes volume that were more than 2-fold upregulated in cornea of *Dscr-1*$^{-/-}$ than WT, of sutured from *Dscr-1*$^{-/-}$ than sutured littermate WT control, and more than 2-fold downregulated in cornea of sutured from DSCR-1 Tg mice compared to sutured littermate WT control. *Red* color means commonly regulated gene set. (**B**) GO pathway analysis of upregulated genes in *Dscr-1*$^{-/-}$ compared to WT (*left*) and suture-mediated DSCR-1 regulatory genes that induced by *Dscr-1*$^{-/-}$ but reduced by DSCR-1 Tg (*right*). *Brown*, *orange*, and *red* indicate immune, cell migration, and

angiogenesis related group, respectively. (**C**) Heatmap representation from the commonly regulated 126 genes. Each gene indicated in left means the highest up or downregulated gene cluster, determined as inflammatory mediated and the Dscr-1 regulated genes. (**C**) mRNA expression of *Sdf-1* in cornea of either WT and *Dscr-1*$^{-/-}$ mice day 5 after sutured (*upper*) or WT and DSCR-1 Tg day 7 after sutured (*lower*), determined by quantitative real-time PCR from the independent specimens. Error bars are the mean ± SD (*P < 0.05). (**D**) Heat map representation from the selected 112 genes that were more than 4-fold upregulated and predominantly expressed in endothelial cells. (**E** and **F**) mRNA expression of *cxcr4* in microvascular endothelial cells from WT and *Dscr-1*$^{-/-}$ (*E*) and WT and DSCR-1 Tg (*F*) mice. Values mean the average differences from two independent microarrays.

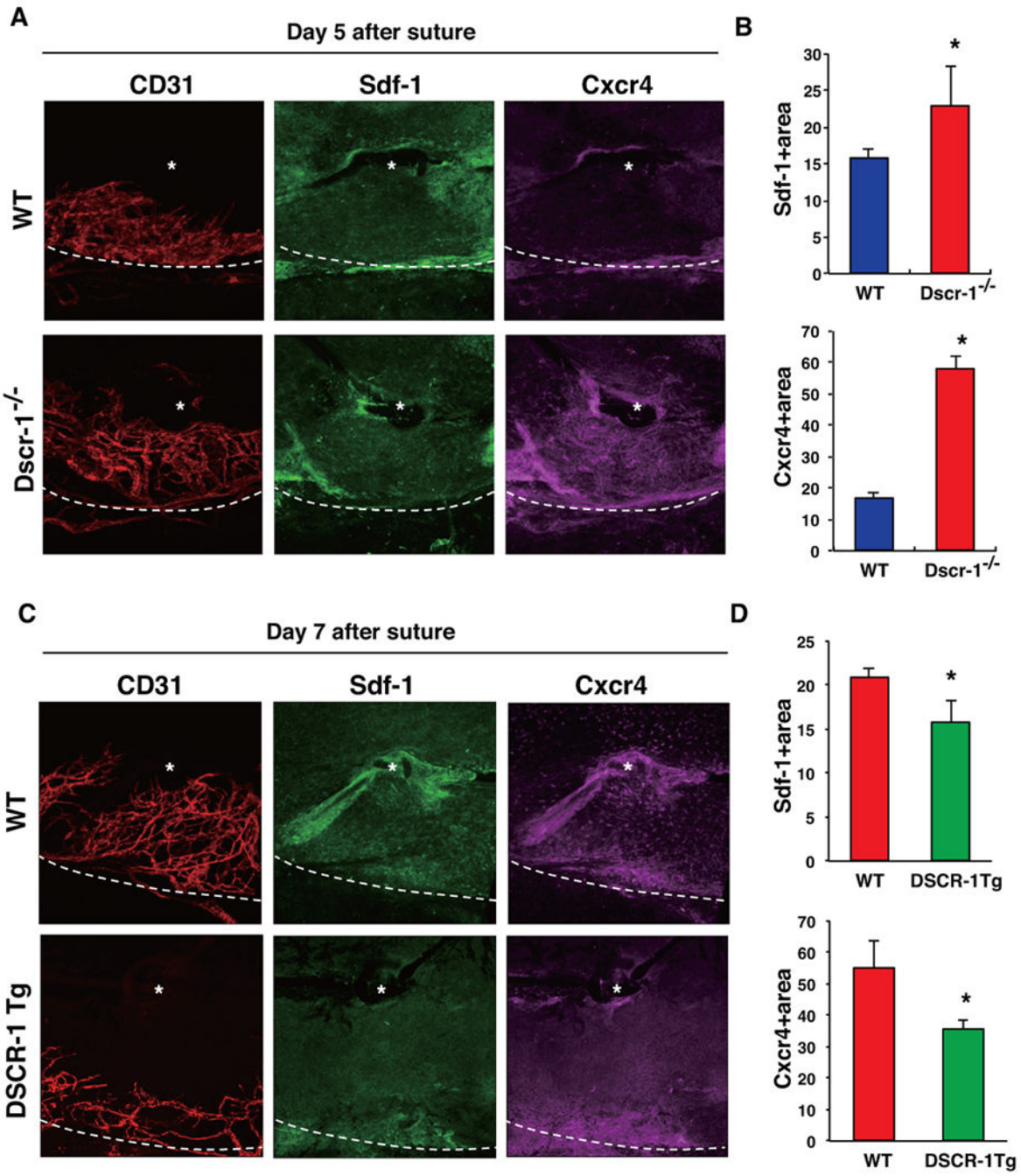

Figure 4. Loss of Dscr-1 increases pro-angiogenic Sdf-1-Cxcr4 signaling axis in cornea.

(**A** and **C**) Representative immunostaining of CD31 (*red*), Sdf-1 (*green*), and Cxcr4 (*purple*) from WT and Dscr-1$^{-/-}$ in day 5 (*A*) or WT and DSCR-1Tg in day 7 (*C*) after suture. Asterisk; sutured area, and broken line; marginal region. (**B** and **D**) Quantification of the Sdf-1 (*upper* graph) or Cxcr4 positive (*lower* graph) area from day 5 (*B*) or day 7 (*D*) after suture. n=5, mean ± SD, *P<0.05 compared with WT (Student's t-test).

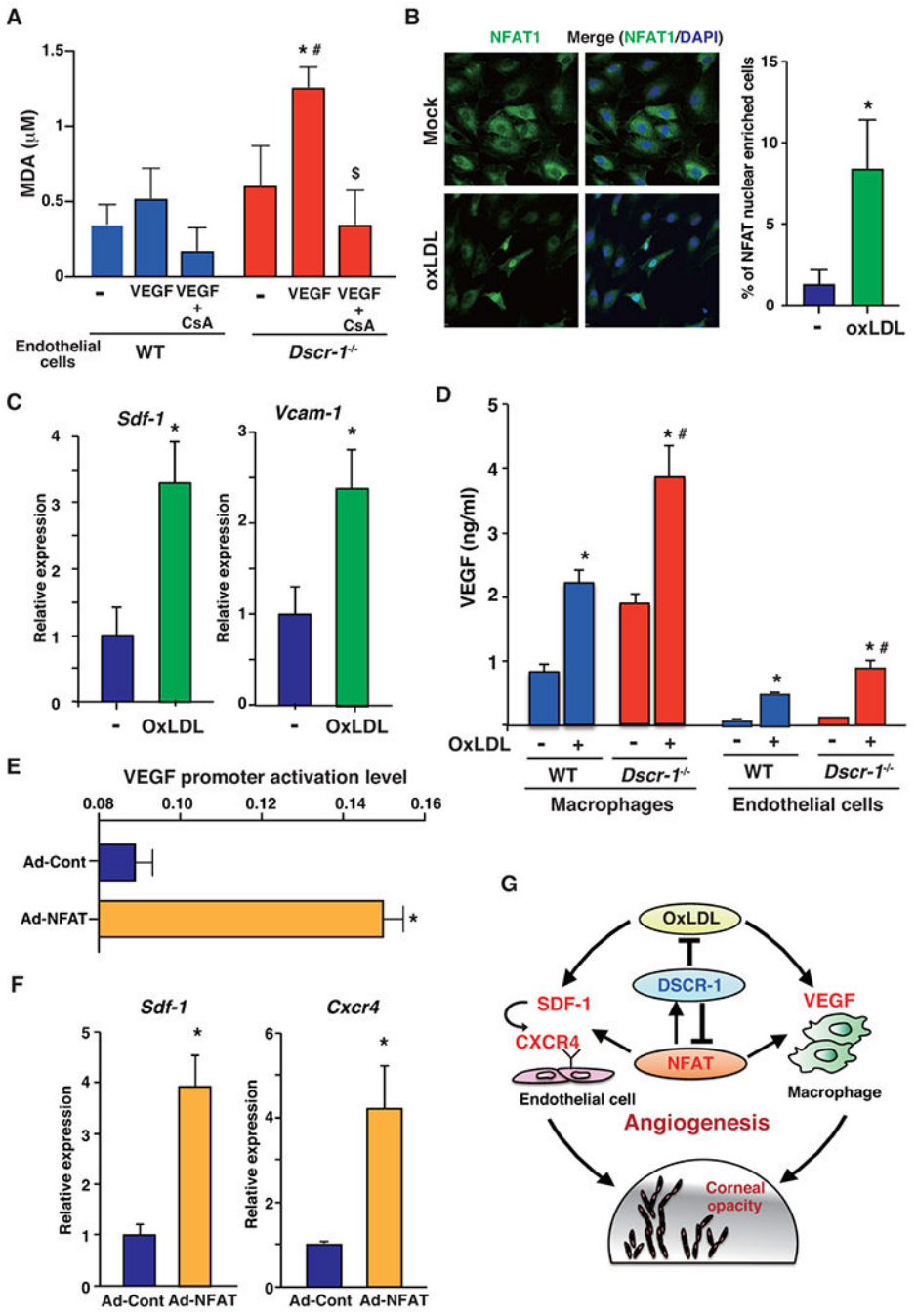

Figure 5. *ApoE* and *Dscr-1* null-mediated oxLDL exaggerated pathological angiogenesis.

(**A**) MDA assay with endothelial cells from WT and *Dscr-1*$^{-/-}$ mice. *, $P<0.01$ compared with VEGF treatment from WT. # and $, $P<0.05$ compared with PBS (−) and VEGF treatment from *Dscr-1*$^{-/-}$, respectively. (**B**) Immunostainings to anti-NFAT1 antibody with microvascular endothelial cells in the presence or absence of 50μg/ml oxLDL. Merged images with DAPI were shown in *right*. Bar graph indicated the nuclear localized NFAT levels. The mean ± SD relative to control were derived from five independent samples.*, $P<0.001$ compared with mock control. (**C**) *Sdf-1* and *vcam-1* mRNA expression in

microvascular endothelial cells. The mean ± SD relative to minus oxLDL control were derived from six independent samples. *, $P<0.05$ compared with mock control. (**D**) VEGF secreted levels in macrophages and endothelial cells from WT or *Dscr-1*$^{-/-}$ mice. The graph value and the ± SD relative to mock control were derived from at least three independent mice. *, $P<0.05$ compared without oxLDL in each mouse. #, $P<0.05$ compared with WT in the presence of oxLDL. (**E**) VEGF promoter activation levels in the adenovirally overexpressed NFAT or the mock control. Values were calculated by luciferase activity described into the methods (n=6). *, $P<0.001$ compared with control. (**F**) *Sdf-1* and *cxcr4* mRNA expression in microvascular endothelial cells in the adenovirally overexpressed NFAT or the mock control. The mean ± SD relative to Ad-control were derived from six independent samples. *, $P<0.05$ compared with control. (**G**) Schematic representation of the corneal pathology model in *Dscr-1* and *ApoE* double null mutation.

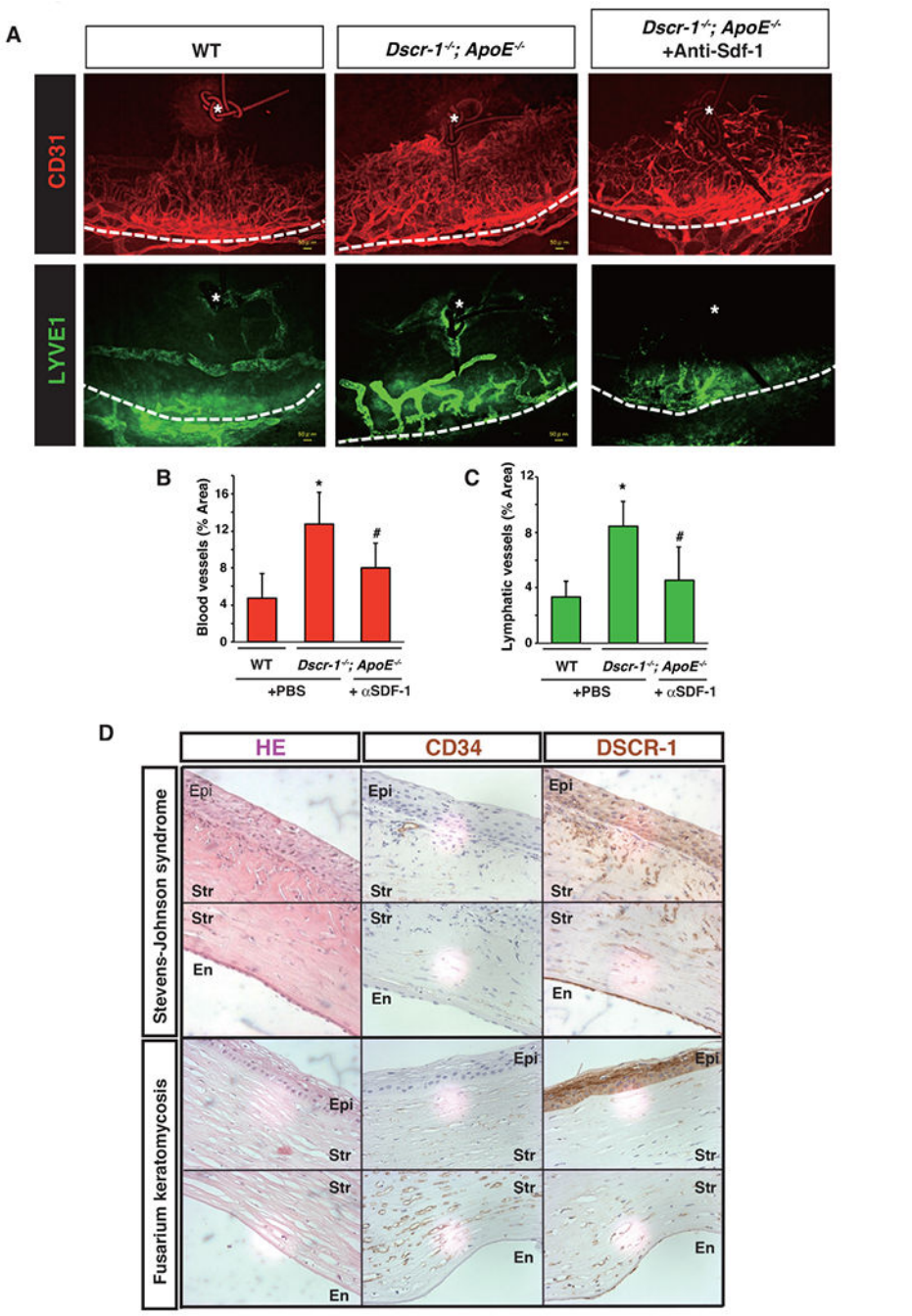

Figure 6. Administration of SDF-1 neutralize antibody attenuated corneal angiogenesis and lymphangiogenesis in intrastromal sutured cornea.

(**A**) Representative angiogenic and lymphangiogenic responses of cornea from WT or *Dscr-1* and *ApoE* combined null mutation mice in the presence or absence of anti-Sdf-1 on day 7 after the intrastromal suturing with 10-0 nylon. (**B** and **C**) Surface areas of corneal angiogenesis (*B*) and lymphangiogenesis (*C*) were quantified with vascularized area versus total corneal area. The mean ± SD were derived from six independent mice. * $P<0.05$ compared with WT in the absence of anti-Sdf-1 treatment. # $P<0.05$ compared with

Dscr-1$^{-/-}$ and *ApoE*$^{-/-}$ in the absence of anti-SDF-1 administration. (**D**) Representative immunohistochemistry for CD34 and DSCR1 (*brown*) in the human patients. Nuclei are counterstained with hematoxylin (*blue*). Upper and lower two jointed figures were from Stevens-Johnson syndrome and Fusarium keratomycosis, respectively. Epi; corneal epithelium, Str; corneal stroma, and En; corneal endothelium.